Quantitative gas saturation estimation by frequency-dependent AVO analysis

Xiaoyang Wu,[1]* Mark Chapman[1,2] Xiang-Yang Li[1], and Patrick Boston[2]

1 Edinburgh Anisotropy Project, British Geological Survey, Murchison House, West Mains Road, Edinburgh EH9 3LA, UK.

2 School of Geosciences, University of Edinburgh, The King's Buildings, West Mains Road, Edinburgh EH9 3JW, UK.

* Corresponding author, E-mail: xywu@bgs.ac.uk

Abstract

Seismic amplitudes contain important information which can be related to fluid saturation. The amplitude-versus-offset (AVO) analysis of seismic data based on Gassmann's theory and approximation of the Zoeppritz equations, has played an central role in reservoir characterization. However, this standard technique faces a long standing problem, its inability to distinguish between partial gas and "fizz-water" with little gas saturation. In this paper, we studied seismic dispersion and attenuation in partially saturated poroelastic media by using frequency-dependent rock physics model, through which the frequency-dependent AVO (FAVO) response is calculated as a function of porosity and water saturation. We propose a crossplotting of two attributes derived from FAVO response to differentiate partial gas saturation and "fizz-water" saturation. One of the attributes is a measure of "low frequency" or Gassmann, reflectivity, while the other is a measure of the "frequency-dependence" of reflectivity. This is in contrast to standard AVO attributes, where there is typically no such separation. A pragmatic FAVO inversion for rock and fluid properties is also established based on Bayesian theorem. Synthetic study is performed to explore the potential of the method to estimate gas saturation and porosity variations. An advantage of our work is that the method is in principle predictive, opening the way to further testing and calibration with

field data. We believe that such work should guide and augment more theoretical studies of FAVO analysis.

Introduction

Reservoir characterization and fluid detection are fundamental goals of geophysical technology. The reliable estimation of gas saturation is a long standing problem (Han and Batzle, 2002), which is important in both exploration and interpretation of time-lapse data. Despite some progress in the application of Bayesian inversion concepts (Bachrach, 2006), reliable estimation of gas saturation has remained elusive. The root of the problem is the relative insensitivity of seismic velocity to gas saturation variations. Introduction of a small amount of gas often leads to a sudden drop in velocity, but only small further variations may be seen when the gas saturation is increased further.

In principle, consideration of attenuation may improve the situation, since the relationship between attenuation and water saturation typically has a different form to that between velocity and water saturation (Murphy, 1982, 1984; Gist, 1994; Cadoret et al., 1998; Nakagawa et al., 2013). Nevertheless, attenuation-based techniques face obstacles in terms of the difficulty of the measurements and the lack of appropriate modelling and interpretation frameworks.

Significant strides have been made recently in the measurement of attenuation from seismic reflection data (Dasgupta and Clark, 1998; Clark et al., 2001; Reine et al 2009). The basis of the techniques is measuring the cumulative loss of energy during transmission through an attenuating zone. The applicability of the method is limited by the thickness of the attenuating zones, and some targets are too thin for successful application of the method. An alternative approach (Chapman et al., 2006; Ren et al., 2009; Wilson et al., 2009; Xu et al., 2011, Zhang, 2011; Innanen, 2011, 2012; Sun et al., 2012; Wu et al., 2013) aims to estimate seismic attenuation indirectly through the frequency-dependence of the reflection coefficient from attenuative and dispersive media.

The frequency-dependence of seismic velocities and attenuations in fluid saturated rocks is the subject of intensive current research from both a theoretical and experimental standpoint (Korneev et al., 2004; Müller and Rothert, 2006; Quintal and Tisato, 2013; Tisato and Quintal, 2013). However, many important aspects remain poorly understood and controversial. It appears that no currently available theory can satisfactorily describe and predict velocity dispersion and attenuation. The case of partially saturation appears to be particularly difficult. In this paper, we investigate the possibility of determining gas saturation from the frequency-dependence of reflectivity in the pre-stack domain using simplified, but we believe representative, rock physics theory. We show how existing frequency-dependent rock physics theory can be used as a tool to match water saturation information at the well to the output of frequency-dependent amplitude-versus-offset analysis of seismic reflection data. Our results are placed in a convenient Bayesian inversion scheme, which allows the theoretical detectability of saturation and porosity variations to be assessed. While future testing on field data is required to validate the technique.

We begin by briefly reviewing the current understanding of seismic dispersion and attenuation in fluid saturated rocks. We then present a pragmatic approach to calculating frequency-dependent reflectivity on the basis of parameters which can be estimated from well log data. The calculated data can then be used as a basis for our Bayesian inversion scheme targeted at recovering porosity and saturation variations. A numerical example illustrates the potential power of the technique.

Modelling attenuation and dispersion in partially saturated rock

The development of mathematical theories to describe the dispersion and attenuation of seismic waves in fluid saturated rock has been a focus of research for over 50 years (Biot, 1956a, 1956b), and the field is still actively developing (Müller et al., 2010). The Biot theory of poroelasticity attempt to describe the behaviour of global flow in fluid-saturated rocks, has

provided an elegant foundation for many studies. The low frequency limiting velocities predicted by Biot theory are consistent with those predicted by the Gassmann equation (Gassmann, 1951), which is still the cornerstone for most studies of fluid substitution in the petroleum industry.

Recently, it has been suggested that the concept of "squirt-flow" (Mavko et al., 1979) describing the microscopic wave induced fluid flow between pores and cracks, provides an important source of additional attenuation, which is not accounted for in the Biot theory (eg. King, 2000). The first mathematical descriptions of squirt-flow were produced in the 1970's (O'Connell & Budiansky, 1977). More recently, the development has proceeded down parallel paths separated by the preferred means of describing the pore space of the rock. One general approach (Mavko & Jizba, 1991; Dvorkin et al., 1995; Pride et al., 2004; Gurevich et al., 2010; Gurevich, 2013) avoids an explicit mathematical description of the pore space, and emphasises the use of averaged, bulk, rock properties. Another approach (Hudson et al., 1996; Pointer et al., 2000; Chapman et al., 2002; Chapman, 2003; Jakobsen et al., 2003; Chapman, 2009, Jakobsen and Chapman, 2009) describes the squirt effect on the basis of inclusion models. Inclusion models benefit from precise mathematical descriptions of the stiffness of pores, but rely on idealized geometries not encountered in nature. The utility of inclusion models has been doubted by Avseth et al. (2004) and others.

In theory, the Biot theory assumes that the period of the seismic wave is sufficiently long to allow local fluid pressure gradients to relax. Squirt-flow theory, by contrast, considers that heterogeneity in the pore structure gives rise to micro-scale fluid pressure gradients which may not be equilibrated by fluid flow on the time scale of the seismic wave. When fluid pressure gradients are un-relaxed, the rock is stiffer than in the relaxed case. This reasoning leads to a pronounced frequency-dependence of seismic velocities, with higher frequencies being associated with higher velocities.

Two major differences between the squirt flow and Biot theories lie in the magnitude of the predicted dispersion and the behaviour of the "characteristic frequency" at which the maximum attenuation occurs. Generally, squirt flow is believed to produce larger and more realistic attenuations than the Biot theory. Both approaches suggest that the characteristic frequency depends on the fluid mobility (defined as the ratio of permeability to fluid viscosity), but the nature of that dependence is very different. In the Biot theory, the characteristic frequency moves higher as the fluid mobility is reduced, but the opposite is the case for the squirt theory. Batzle et al. (2006) tentatively suggest that laboratory measurements agree with the squirt theory in terms of the dependence on fluid mobility.

When the rock is partially saturated, further complications ensue. In a landmark study, White (1975) gave a description of how the existence of gas patches give rise to large attenuations. White's model predicts no attenuation or dispersion in the absence of a second fluid. Dutta and Ode (1979) extended White's approach within the framework of Biot theory. Mavko and Mukerji (1998) describe the effect of "patchy saturation", and show that this concept gives rise to increased velocity dispersion. Recently, the role of the scale length of the heterogeneities has also emerged as an important concept, with meso-scale structures (smaller than the wavelength but larger than the grain scale) being associated with dispersion in the seismic frequency band. This phenomenon has been studied through numerical modelling (Rubino and Holliger, 2012; Quintal and Tisato, 2013).

Laboratory measurements (Murphy, 1982; Murphy, 1984; Cadoret et al. 1984) suggest that attenuations for small partial gas saturation are higher than for the fully saturated case. Gist (1994) presents laboratory measurements on partially saturated rock and argues that their interpretation requires a unified model with both the "squirt-flow" and "gas pocket" effects. Unfortunately, no truly satisfactory such model yet exists. Recently, Amalokwu et al. (2014) present measurements of attenuation versus water saturation in fractured and unfractured

rocks which appear to be a severe challenge to currently developed theory. The development of models for partially saturated rock is currently a focus of intensive research.

Given the uncertainty in the underlying rock physics, and the absence of a satisfactory modelling approach, it is tempting to conclude that application of the concepts to the interpretation of seismic data is currently impossible, and that progress must await the development of more advanced theories. This paper explores the opposite point of view, presenting a pragmatic approach to the application of existing theory to infer variations in porosity and saturation.

Our approach is based on three key assumptions. Firstly, we assume that the behaviour of the rock is consistent with the Gassmann-Wood predictions at low frequency. We further assume that partial gas saturation generally gives higher values of attenuation than full saturation, with maximum values of attenuation occurring for low gas saturation. Lastly, we assume that the dependence of the characteristic frequency on fluid mobility follows the predictions of the squirt-flow theory.

We show below that it is possible using existing theory to provide a modelling scheme which is broadly consistent with these assumptions. We do not claim to be able to predict *a priori* values of attenuation associated with a given water saturation. Rather, we aim to provide a modelling framework which is capable of being calibrated when both seismic data and water saturation information from log data are available. In this way, we hope that our model may provide useful information even when the precise details of the attenuation mechanisms may not be fully understood.

Method for the calculation of frequency-dependent reflectivity

We base our calculations on poroelastic rock physics model presented by Chapman et al. (2002). The model is primarily a squirt flow theory considering the fluid exchange between pores and cracks, as well as between cracks of different orientations due to wave propagation.

Chapman et al. (2002) discussed the consistency of the model with Gassmann's relations, which is an advantage in the current context. We propose to use the model in conjunction with an effective single-phase fluid model. This produces what may be a reasonable qualitative relationship between attenuation and water saturation, but it should be borne in mind that this set up rules out many of the partial saturation attenuation mechanisms which have been discussed in the literature. Following the theory of Chapman et al.(2002), the frequency-dependent effective bulk and shear moduli K_{eff} and μ_{eff} are expressed as follows:

$$K_{eff} = K - v\left\{\frac{4(3\} + 2\sim)(\} + 2\sim)}{\sim(\} + \sim)}[1 - 3A(\check{S})] - 4frA(\check{S})\right\}$$
$$- w\left\{\frac{3\} + 2\sim}{4\sim}\left[\frac{\} + 2\sim}{3\} + 2\sim} + B(\check{S})\right] - 3B(\check{S})\right\} \tag{1}$$

$$\sim_{eff} = \sim - \frac{16}{45}v\frac{1}{1 + K_c}\frac{\sim(\} + 2\sim)}{3\} + 4\sim}\left(K_c + \frac{1}{1 + i\check{S}\ddagger}\right) - \frac{32}{45}v\frac{\sim(\} + 2\sim)}{3\} + 4\sim}$$
$$- w\frac{15\sim(\} + 2\sim)}{9\} + 14\sim} \tag{2}$$

where   is the angular frequency, K, μ,   denote the bulk and shear moduli and Lame parameter of the solid mineral matrix respectively, while the fluid bulk modulus is K_f, the total porosity is w . r, a,   are the aspect ratio, uniform crack radius and crack density of the cracks respectively. *A* and *B* are:

$$A(\check{S}) = \frac{(1 + i\check{S}x\ddagger)\frac{\} + 2\sim}{\} + \sim}\left[\frac{16v}{27w(1 + K_p)} + \frac{\} + \sim}{3\} + 2\sim}\right] + i\check{S}\ddagger\left[\frac{1}{3(1 + K_c)} - x'\right]}{1 + i\check{S}\ddagger + (1 + i\check{S}x\ddagger)\frac{16v(1 + K_c)}{9w(1 + K_p)}\frac{\} + 2\sim}{\} + \sim}} \tag{3}$$

$$B(\check{S}) = \frac{\frac{1}{3(1 + K_c)} + \frac{9(1 + K_p)}{16(1 + K_c)}\frac{\} + \sim}{3\} + 2\sim} + \frac{i\check{S}\ddagger}{1 + i\check{S}\ddagger}\left[x' - \frac{1}{3(1 + K_c)}\right]}{\frac{9(1 + K_p)}{16(1 + K_c)}\frac{\} + \sim}{\} + 2\sim} + \frac{1 + i\check{S}x\ddagger}{1 + i\check{S}\ddagger}} \tag{4}$$

$$x' = x\frac{\} + 2\sim}{(3\} + 2\sim)(1 + K_p)} \tag{5}$$

$$\chi = \frac{3f(\} + \sim)(1 + K_p)}{4(\} + 2\sim)(1 + K_c)} \qquad (6)$$

$$K_p = \frac{4\sim}{3K_f} \qquad (7)$$

$$K_c = \frac{f\sim r(\} + \sim)}{K_f(\} + 2\sim)} \qquad (8)$$

where   is the timescale parameter that controls the frequency regime over which the dispersion occurs.

When saturating fluid is an mixture of gas and water, density of the partially saturated sandstone ($_{sat}$) used in the model was calculated as,

$$\cdots_{sat} = \cdots_m(1-w) + w\cdots_f \qquad (9)$$

$$\cdots_f = S_g\cdots_g + (1-S_g)\cdots_w \qquad (10)$$

where $_m$, $_f$, $_g$, $_w$ is the densities of rock matrix, effective fluid, gas and water respectively. S_g is gas saturation. The bulk modulus of mixed fluid K_f is estimated by Wood's formula,

$$K_f = \frac{1}{S_g / K_g + (1 - S_g)/K_w} \qquad (11)$$

K_g and K_w are the bulk moduli of gas and water respectively. Viscosity of the effective single-phase fluid is averaged arithmetically in term of volume percentage. Thus, viscosity and bulk modulus of the effective fluid change with gas saturation S_g. This can further changes attenuation due to squirt flow. After frequency-dependent elastic moduli has been derived, frequency-dependent PP wave reflectivity can be calculated using the anisotropic Zoeppritz equation generalized by Schoenberg and Protazio (1992, see Appendix I).

Table 1 displays the parameters of a two-layer model with shales overlying sandstone reservoir. The lower layer is considered to be dispersive. Figure 1 displays the attenuation curves varying with (a)frequency, (b)gas saturation at different porosities, and (c)crack densities, for the lower layer using the theory of Chapman et al.(2002). As shown in Figure 1

(a) and (b), attenuation peaks at about 50Hz, with a corresponding Q value of 16. Figure 1(b) shows that low attenuation is predicted for full saturation by either fluid, with a maximum of attenuation occurring at an intermediate saturation and minimum of attenuation for full gas saturation. The location of the maximum attenuation is model dependent, but usually occurs for gas saturations between 10% and 50%, with a bias towards low gas saturations. Figure 1(c) shows the maximum value of attenuation is also sensitive to the "crack density" parameter. This parameter can be used to modulate the frequency-dependence of reflectivity and calibrate to the real data.

Figure 2 displays the frequency-dependent PP-wave reflection coefficients when varying water saturation from 100% to 0% every 20%. The interface has high-to-low P-wave impedance with Class III AVO response. We can see that with the increasing of gas saturation, the value of reflectivity become larger. An obvious characteristic is these plots illustrate nearly no dispersion at full gas saturation(f), slight dispersion at full water saturation (a) and considerable frequency dependence at partial saturation. This reflectivity behaviour is consistent with the predicted attenuation as shown in Figure 1(b). It is worth to mention that, for partial gas saturation, the zero offset variation of reflection coefficient due to frequency is 0.015, which is significant in comparison to the variation with offset over the 40° range (0.05 when Sw=60% at 10Hz). This indicates that the variation of reflection coefficients due to dispersion is significant in partially saturated sand.

Spectral decomposition and balancing

For real seismic data, spectral decomposition techniques may be used to calculate the spectral amplitude at different frequencies. A variety of spectral decomposition techniques, such as STFT (Short Time Fourier Transform, Partyka et al., 1999), CWT (Continuous Wavelet Transform, Sinha et al, 2005), MPD (Matching Pursuit Decomposition, Wang et al., 2007), WVD (Wigner-Ville Distribution, Wu and Liu, 2009) based methods, have been studied and

used for different applications. Spectral decomposition transforms seismic amplitudes, $D(t, n)$, at time t and receiver n into spectral amplitudes, $S(t, n, f)$, at frequency f such that,

$$D(t, n) \quad S(t, n, f) \qquad (12)$$

Afterwards, spectral balancing should be performed on the spectral amplitude to remove the overprint effect of source wavelet (Partyka *et al*., 1999) if the true spectral behaviour of the geology and saturating fluid is desired. Various methods such as spectral *L-p* norm scaling (Marfurt and Kirlin, 2001), spectral stabilisation (Burnett *et al*., 2003) and spectral balancing (Odebeatu *et al*., 2006; Wilson, 2009) have been proposed. We remove the effect of the source wavelet by designing a suitable weight function $w(\mathrm{n}, f)$,

$$B(t, n, f) = S(t, n, f)w(n, f) \qquad (13)$$

$w(n, f)$ is calculated from a defined window with k sampling points using the ratio of RMS amplitudes at the chosen reference frequency f_0 and other frequencies as following,

$$w(f, n) = \frac{\sqrt{\sum_k S^2(t, n, f_0)}}{\sqrt{\sum_k S^2(t, n, f)}} \qquad (14)$$

Then the amplitudes at different frequencies become comparable. We consider a two-layer Class III P-wave AVO model presented by Chapman et al. (2005), where the top elastic layer had P- and S-wave velocities of 2743m/s and 1394m/s. For the dispersive model, the lower layer is defined as a material under water-saturation then substituted with gas by changing the fluid bulk modulus from 2GPa to 0.2GPa. For the elastic model, the P- and S-wave velocities of lower layer were calculated from elastic tensor for the dispersive model at low frequency. Eleven traces for each model are generated using 40Hz Ricker wavelet as the source. The trace space is 100m.

Figure 3 displays the synthetic gathers of the elastic and dispersive models at the interface respectively, both of which the amplitudes increase with the offset gradually. However, compared with the elastic model, the amplitudes for the dispersive model have decreased.

The WVD based spectral decomposition method is performed to calculate the spectral amplitudes at 25, 30, 40, 50, 60, 70 and 80Hz.

A set of weights are derived in the elastic model by matching the peak amplitude of the isofrequency trace to the 40Hz amplitude to remove the overprint of source wavelet. These same weights are applied to the dispersive model. Figure 4 shows a comparison of isofrequency sections between the elastic and dispersive models at 25, 40, 60 and 80Hz. For the elastic model (upper), similar energy appears on each isofrequency section after spectral balance, while for the dispersive model (lower), energy reduces at 25Hz as opposed to elastic model and decreases significantly with the increase of frequency.

FAVO attributes

AVO attributes (such as intercept, gradient, fluid factor) have been derived from standard AVO analysis and provided useful fluid information. Analogously, we expect to derive attributes which can delineate fluid information from FAVO analysis. Wilson et al. (2009)'s FAVO inversion produces an attribute that measured the frequency-dependence of reflectivity. Clearly, it would be advantageous to be able to quantitatively relate such attribute to rock properties of interest.

Our attention is focussed on the particular rock property of interest. We design a two-layer model with elastic shale overlying fluid-saturated dispersive sandstone. Following the theory of Boston (2011), the reflectivity at the interface is calculated as a function of rock property (for instance, gas saturation) frequency and offset. The reflection coefficients of p different values of gas saturation X_k ($k=1,2,\ldots,p$), m angles of incidence θ_i ($i=1,2,\ldots,m$), n frequencies f_j ($j=1,2,\ldots,n$) are calculated, and then spliced together into a large matrix of the following form:

$$R = \begin{bmatrix} R^{f_1}_{\theta_1} & \cdots & R^{f_n}_{\theta_1} & R^{f_1}_{\theta_1} & \cdots & R^{f_n}_{\theta_1} & \cdots & R^{f_1}_{\theta_1} & \cdots & R^{f_n}_{\theta_1} \\ R^{f_1}_{\theta_2} & & R^{f_n}_{\theta_2} & R^{f_1}_{\theta_2} & & R^{f_n}_{\theta_2} & & R^{f_1}_{\theta_2} & & R^{f_n}_{\theta_2} \\ \vdots & & \vdots & \vdots & & \vdots & & \vdots & & \vdots \\ R^{f_1}_{\theta_m} & \cdots & R^{f_n}_{\theta_m} & R^{f_1}_{\theta_m} & \cdots & R^{f_n}_{\theta_m} & \cdots & R^{f_1}_{\theta_m} & \cdots & R^{f_n}_{\theta_m} \end{bmatrix}$$

$$\underbrace{\qquad}_{X_1} \ \cdots\cdots \ \underbrace{\qquad}_{X_2} \ \cdots\cdots\cdots \ \underbrace{\qquad}_{X_p}$$

(15)

Following the method of Causse et al. (2007) and Varela et al. (2009), the singular value decomposition (SVD) is performed on the matrix. This allows us to approximate the reflection coefficients as a series of weights C, which are a function of rock property X and frequency f, and basis functions h are a function of angle of incidence:

$$R^{f_j}_{X_k}(\theta_i) \approx C_1(f_j, X_k)h_1(\theta_i) + \cdots + C_i(f_j, X_k)h_i(\theta_i) \tag{16}$$

The dependence of the weight functions on frequency can be approximated by a linear relationship,

$$C_i(f_j, X_k) = CO_i + (f_j - f_1)dC_i(X_k) \tag{17}$$

This gives rise to a forward modelling which allows us to carry out intercept-gradient analysis for the frequency-dependent reflectivity of each rock property. The intercept attribute is a measure of the "low frequency" reflectivity, while the gradient attribute is a measure of the frequency-dependence of reflectivity, which is similar to the attribute by Wilson et al.(2009). Crossplotting the two attributes may help us differentiate different gas saturation scenarios.

We apply this method to the two-layer model used by Rutherford and Williams (1989). The lower layer is considered to be saturated with effective fluid of gas and water, where dispersion and attenuation are introduced. Gas saturation is the reservoir property of interest. The material parameters for the model are listed in table 2.

The reflection coefficients matrix R are calculated for 15 scenarios of gas saturation, 5 cases from 1% to 5% with a step of 1%, and the other 10 cases from 10% to 100% with a step of 10%. Then the "intercept-gradient" crossplot can be generated by the foregoing method.

Figure 5 displays the crossplot of the two attributes. It indicates that the intercept attribute increase with gas saturation. Peak value of the attribute measures "frequency-dependence of reflectivity" at 5% of gas saturation. From this crossplot, partial gas saturation (larger than 10% and smaller than 50%) and "fizz water" saturation (larger than 1% and smaller than 10%) are clearly separated.

Bayesian inversion using FAVO analysis

The Bayesian theorem in terms of probability density functions (pdf) can be written as

$$P(m\,|\,d) = \frac{P(d\,|\,m)P(m)}{P(d)}$$ (18)

where $P(m\,|\,d)$ is the pdf of model parameters m when giving the observing data d. $P(d\,|\,m)$ is the pdf of d when given m, which is also known as likelihood function. It measures the misfit between the forward modelling data r derived from m and the observing data d. High misfit between r and d will give small likelihood. $P(m)$ is the prior information. $P(d)$ can be considered as a constant since the data d is observed. Here, we propose a model-based FAVO inversion technique to estimate porosity and gas saturation from analyses of well logs and pre-stack seismic data, which has the merit of being readily applicable to field data. The main steps are as follows:

(i) Spectrally decomposing and balancing pre-stack data along the reservoir position to obtain the spectral amplitudes d varying with angle of incident θ_i at frequencies f_j,

$$d = d(\theta_i, f_j).$$ (19)

(ii) Deriving a starting background model for both upper and lower layers from well log data. This includes representative values of V_p, V_s and density, or distributions of values, associated with given petrophysical parameters such as porosity ϕ and water saturation S_w.

(iii) Calculating the attenuation and frequency-dependent reflection coefficient r for each realisation of the petrophysical parameters using the parameters derived in step (ii),

$$r = r(\phi_i, f_j). \tag{20}$$

(iv) Comparing r with d, and calculate the misfits between them. This provides a basis for an inversion of the data in terms of petrophysical parameters.

(v) Using Bayesian theorem to estimate the probability of each scenario of petrophysical parameters. For estimating the posterior probability of ϕ and S_w when given the observed spectral amplitudes d:

$$P(\{\phi, Sw \mid d) = \frac{P(d \mid \{\phi, Sw)P(\{\phi, Sw)}{P(d)}, \tag{21}$$

The prior probability $P(\phi, S_w)$ can be derived from statistical analysis of well log data. $P(d \mid \phi, S_w)$ is the likelihood function. We use an empirical relation to estimate $P(d \mid \phi, S_w)$:

$$P(d \mid \{\phi, Sw) \propto \exp(-s \cdot \Delta E), \tag{22}$$

where s is a constant, ΔE is the sum of absolute error between forward modelling reflectivities $g(\phi, S_w)$ and d at each incident angle.

$$\Delta E = \sum_i \sum_j \left| d - g(\{\phi, Sw) \right|. \tag{23}$$

Equation (21) illustrates that the posterior probability depends on both prior information and likelihood function. We use the parameters in Table 1, and assume 60% water saturation in the pores to perform a synthetic study. Under such case, the characteristic frequency is 31Hz and 11.76 for corresponding Q value. Figure 6 displays the frequency-dependent reflectivity and phase for the two-layer model. The high-to-low interface gives rise to Class III AVO with phase around 180 degree. The value of reflectivity is higher with increasing of frequency. Since the spectral amplitude of a seismic signal become positive value, we consider the amplitude value without phase effect. 10% Gaussian random noise was added into the reflectivity as the "observing data". Then, we can study the potential resolution of the method for determining variations in porosity and saturation.

We then scan through different combinations of porosity and water saturation S_w, and compute misfit between the theoretical reflectivity and the "observing data". This analysis is repeated by replacing the frequency-dependent modelling with the single frequency approach. The derived misfits can be transformed to likelihood function by using equation (22). Figure 7 displays the likelihood functions, the well known result that it is hard to distinguish between low and high gas saturations on the basis of Gassmann theory is recovered (b), but the frequency-dependent theory shows more promising (a). The reason for this result is that while high and intermediate gas saturations show the same reflectivity for low frequencies, the frequency-dependence of the reflectivity is different because of the behaviour depicted in Figure 1. Figure 7(a) shows that the maximum likelihood occurs at 16% porosity and 55% water saturation. The deviation of water saturation from true value (60%) is due to the Gaussian random noise added into the "observing data". Three other local maximum likelihood values also occur. This indicates that increase in porosity and water saturation to a certain extent may have similar seismic response, which leads to multi-solutions of petrophysical parameters. Figure 8 shows the fitting results at the maximum likelihood for (a) frequency-dependent case and (b) Gassmann case.

Finally, normal distributions of $N(0.1, 0.25)$ for porosity and $N(0.9, 0.25)$ for water saturation are assumed respectively as the prior information. Figure 9 displays the prior probability of porosity and water saturation. Figure 10 displays the posterior probability, which is calculated by multiplying the likelihood functions with the prior information. The frequency-dependent theory (a) provides more accurate inversion of porosity and saturation than Gassmann theory (b). The similar procedure can be applied to seismic data for different locations. Seismic data is compared to the theoretical response for different combinations of porosity and saturation. As such, this technique can be used to assess the likely changes in porosity and saturation between zones where seismic data are available.

Conclusions

In this paper, we have discussed the feasibility of using FAVO response for quantitative estimation of gas saturation. The Frequency-dependent rock physics model is combined with reflectivity method to calculate the reflectivity that is incident angle, frequency and reservoir properties (porosity and saturation) dependent. A crossplot of two FAVO attributes is derived using singular value decomposition, one measured the reflectivity at low frequency and (intercept) the other measured the frequency-dependence of reflectivity (gradient). Numerical study demonstrates that crossplotting of the two attributes is able to differentiate the three cases of full gas saturation, full water saturation and partial gas saturation.

A Bayesian inversion of porosity and saturation is also introduced based on FAVO response. Through synthetic modelling studies, we have demonstrated that the Bayesian inversion of FAVO response is theoretically capable of providing more quantitative estimation of petrophysical parameters than the standard AVO techniques. In real data processing, the field data can be decomposed and balanced into a set of spectral amplitudes, while the parameter "crack density" can be used to modulate the frequency-dependence of reflectivity and calibrate the theoretical reflectivity to real spectral amplitudes. It is worth to mention that not only suitable for attenuation due to squirt flow, our methodology of estimation gas saturation also applies to cases where other dispersive mechanisms (such as patchy saturation) give rise to velocity dispersion. Hence, we argue that it may be possible to estimate gas saturation from FAVO response with suitable processing and analysis of seismic data.

Acknowledgements

References

Amalokwu, K., Best, A., Sothcott, J., Chapman, M., Minshull, T. & Li, X-Y. 2014. Water saturation effects on elastic wave attenuation in porous rocks with aligned fractures. Geophysical Journal International, 197(2), 943-947.

Avseth, P., Mukerji, T., & Mavko, G., 2005, Quantitative seismic interpretation - Applying rock physics tools to reduce interpretation risk, Cambridge University Press.

Bachrach, R., 2006. Joint estimation of porosity and saturation using stochastic rock-physics modelling. Geophysics, 71(5), O53-O63.

Batzle, M.L., Han, D.-H. & Hofmann, R., 2006. Fluid mobility and frequency-dependent seismic velocity, direct measurements, Geophysics, 71(1), N1-N9.

Biot, M. A., 1956a, Theory of propagation of elastic waves in fluid-saturated porous solid. I. Low-frequency range: Journal of the Acoustical Society of America, 28, 168-178.

Biot, M. A., 1956b, Theory of propagation of elastic waves in a fluid-saturated porous solid. II. Higher frequency range: Journal of the Acoustical Society of America, 28, 179-191.

Boston P., 2011. Rock physics model-based derivation of gas saturation from Frequency-dependent Amplitude-Versus-Offset (FAVO) data, BSc Dissertation, University of Edinburgh.

Burnett, M.D., Castagna, J.P., Méndez-Hernández, E., Rodríguez, G.Z., García, L.F., Vázquez, J.T.M., Avilés, M.T. & Villaseñor, R.V., 2003. Application of spectral decomposition to gas basins in Mexico. The Leading Edge, 22, 1130-1134.

Cadoret, T., G., Mavko, T., G., & Zinszner, B., 1998. Fluid distribution effect on sonic attenuation in partially saturated limestones, Geophysics, 63,154-160.

Causse, E., Riede, M., van Wijngaarden, A.J., Buland, A., Dutzer, J.F. & Fillon, R., 2007. Amplitude analysis with an optimal model-based linear AVO approximation: Part I - Theory. Geophysics, v. 72(3), C59-C69.

Chapman, M., Zatsepin, S.V. & Crampin, S., 2002. Derivation of a microstructural poroelastic model, Geophysical Journal International, 151, 427-451.

Chapman, M., 2003. Frequency dependent anisotropy due to meso-scale fractures in the presence of equant porosity, Geophys. Prospect., 51, 369-379.

Chapman M. & Liu, E., 2003. The frequency dependent azimuthal AVO response of fractured rock, 73rd SEG Annual Meeting, Expanded. Abstracts, 105-108.

Chapman, M., Liu, E., & Li, X.-Y., 2006. The influence of fluid-sensitive dispersion and attenuation on AVO analysis, Geophysical Journal International, 167, 89-105.

Chapman, M. 2009. Modeling the effect of multiple sets of mesoscale fractures in porous rock on frequency-dependent anisotropy, Geophysics. 74, 6, D97-D103

Clark, R. A., A. J. Carter, P. C. Nevill, & P. M. Benson, 2001, Attenuation measurements from surface seismic data - Azimuthal variation and time-lapse case studies: 63rd Conference and Technical Exhibition, EAGE, Expanded Abstracts, L28.

Dasgupta, R. & Clark, R., 1998. Estimation of Q from surface seismic reflection data, Geophysics, 63(6), 2120 - 2128.

Dutta, N. C., & Odé, H., 1979a, Attenuation and dispersion of compressional waves in fluid-filled porous rocks with partial gas saturation (White model) - Part I: Biot theory, Geophysics, 44(11), 1777-1788.

Dutta, N. C., & Odé, H., 1979b. Attenuation and dispersion of compressional waves in fluid-filled porous rocks with partial gas saturation (White model)-Part II: Results, Geophysics, 44(11), 1789-1805.

Dvorkin, J., G. Mavko, & A. Nur, 1995, Squirt flow in fully saturated rocks: Geophysics, 60, 97-107.

Endres, A.L. & Knight, R.J., 1997. Incorporating pore geometry and fluid pressure communication into modeling the elastic behaviour of porous rocks, Geophysics, 62, 106-117.

Gassmann, F., 1951, Über die Elastizität poröser Medien: Vierteljahrsschrift der Naturforschenden Gesellschaft in Zürich, 96, 1-23.

Gist, G. A., 1994. Interpreting laboratory velocity measurements in partially gas-saturated rocks: Geophysics, 59, 1100–1109.

Gurevich, B., Makarynska, D., de Paula, O., & Pervukhina, M., 2010. A simple model for squirt-flow dispersion and attenuation in fluid-saturated granular rocks. Geophysics. 75 (6): pp.N109-N120.

Gurevich, B. 2013, Rigorous bounds for seismic attenuation and dispersion in poroelastic Rocks: EAGE Workshop on Seismic Attenuation, Singapore, O03.

Han, D.-H., & Batzle, M. 2002, Fizz water and low gas-saturated reservoirs: The Leading Edge, 21, 395-398.

Hudson, J. A., E. Liu, & S. Crampin, 1996, The mechanical properties of materials with interconnected cracks and pores: Geophysical Journal International, 124, 105-112.

Innanen, K.A., 2011. Inversion of the seismic AVF/AVA signatures of highly attenuative targets. Geophysics, 76(1), R1-R14.

Innanen, K.A., 2012. Anelastic P-wave, S-wave and Converted-wave AVO Approximations: 74th EAGE Conference & Exhibition, Extended Abstracts, P197.

Jakobsen, M., Hudson, J. A., & Johansen, T. A., 2003. T-matrix approach to shale acoustics. Geophysical Journal International, 154, 533-558.

Jakobsen, M., Chapman, M., 2009, Unified theory of global and squirt flow in cracked porous media. Geophysics, 74, WA65-WA76.

King, M. S., J. R. Marsden, & J. W. Dennis, 2000, Biot dispersion for P- and S-wave velocities in partially and fully saturated sandstones: Geophysical Prospecting, 48, 1075-1089.

Marfurt, K.J. and Kirlin, R.L., 2001. Narrow-band spectral analysis and thin-bed tuning. Geophysics, 66, 1274-1283.

Mavko, G., Kjartansson, E., & Winkler, K., 1979. Seismic wave attenuation in rocks. Rev. Geophysics., 17,1155-1164

Mavko, G., and D. Jizba, 1991, Estimating grain-scale fluid effects on velocity dispersion in rocks: Geophysics, 56, 1940-1949.

Mavko, G., and T. Mukerji, 1998, Bounds on low frequency seismic velocities in partially saturated rocks: Geophysics, 63, 918–924.

Müller T. M., & E. Rothert, 2006. Seismic attenuation due to wave-induced flow: Why Q in random structures scales differently, Geophysical Research Letters, VOL. 33, L16305.

Müller T. M., Gurevich B. & Lebedev M., 2010. Seismic wave attenuation and dispersion resulting from wave-induced flow in porous rocks–A review, Geophysics, 75, A147–A164.

Murphy, W.F., 1982. Effects of partial water saturation on attenuation in massilon sandstone and vycor porous glass, Acoust. Soc. Am. J., 71, 1458–1468.

Murphy, W.F., 1984. Acoustic measures of partial gas saturation in tight sandstones, J. geophys. Res., 89, 11549–11560.

Nakagawa, S., Kneafsey, T. J., Daley, T. M., Freifeld, B. M. & Rees, E. V., 2013. Laboratory seismic monitoring of supercritical CO2 flooding in sandstone cores using the Split Hopkinson Resonant Bar technique with concurrent x-ray Computed Tomography imaging: Geophysical Prospecting, 61, 254-269.

O'Connell, R.J. and Budiansky, B., 1977. Viscoelastic properties of fluid-saturated cracked solids. J.Geophys.Res., 79, 4626-4627.

Odebeatu, E., Zhang, J., Chapman, M., Liu, E. & Li, X.Y., 2006. Application of spectral decomposition to detection of dispersion anomalies associated with gas saturation. The Leading Edge, 25, 206-210.

Partyka, G.A., Gridley, J.M., & Lopez, J., 1999. Interpretational applications of spectral decomposition in reservoir characterization. The Leading Edge 18 (3), 353-360.

Pride S. R., Berryman J. G. & Harris J. M., 2004. Seismic attenuation due to wave induced flow, Journal of Geophysical Research, 109, B01201.

Pointer T., Liu E. and Hudson J.A. 2000. Seismic wave propagation in cracked porous media. Geophysical Journal International 142, 199–231.

Quintal, B. and Tisato, N., 2013. Modeling Seismic Attenuation Due to Wave-Induced Fluid Flow in the Mesoscopic Scale to Interpret Laboratory Measurements. Fifth Biot Conference on Poromechanics, Vienna, pp. 31-40.

Reine, C., van der Baan, M. & Clark, R., 2009. The robustness of seismic attenuation measurements using fixed-and variable-window time-frequency transforms, Geophysics, 74(2), WA123 - WA135.

Ren H., Goloshubin G. & Hilterman F., 2009. Poroelastic analysis of amplitude-versus-frequency variations, Geophysics, 72, N41–N48.

Rubino, J. G., & Holliger, K. 2012, Seismic attenuation and velocity dispersion in heterogeneous partially saturated porous rocks: Geophysical Journal International, 188, 1088-1102.

Rutherford, S.R. & Williams, R.H., 1989. Amplitude-versus-offset variations in gas sands. Geophysics, 54, 680-688.

Sun, S., Jiang, S., Sun, X., Yang, H., Han, J., & Li, Y., 2012. Fluid identification using frequency-dependent AVO inversion in dissolution caved carbonate reservoir. 82nd SEG Technical Program Expanded Abstracts 2012, pp.1-5.

Schoenberg, M. and Protazio, J., 1992. 'Zoeppritz' rationalized and generalized to anisotropy. Journal of Seismic Exploration, 1, 125-144.

Sinha, S., P. S. Routh, P. D. Anno, & J. P. Castagna, 2005. Spectral decomposition of seismic data with continuous-wavelet transform. Geophysics, 70(6), 19-25.

Tisato, N and Quintal, B., 2013. Measurements of seismic attenuation and transient fluid pressure in partially saturated Berea sandstone: Evidence of fluid flow on the mesoscopic scale, Geophysical Journal International, 195(1), 342-351.

Varela, I., Maultzsch, S., Chapman, M. & Li, X-Y., 2009. Fracture density inversion from a physical geological model using azimuthal AVO with optimal basis functions. 79th SEG Annual Meeting Expanded Abstracts, 2075-2079.

Wang, Y., 2007, Seismic time-frequency spectral decomposition by matching pursuit. Geophysics, 72(1), 13-20.

White, J. E., 1975. Computed seismic speeds and attenuation in rocks with partial gas saturation, Geophysics, 40, 224-232.

Wilson, A., Chapman, M., & Li, X-Y., 2009. Frequency-dependent AVO inversion, 79th annual SEG meeting Expanded Abstracts, 28, 341-345.

Wu, X., & Liu, T., 2009. Spectral decomposition of seismic data with reassigned smoothed pseudo Wigner-Ville distribution, Journal of Applied Geophysics, 68(3), 386-393.

Wu, X., Chapman, M., Li, X.-Y., Angerer, E. & Boston P., 2013. Bayesian inversion for porosity and saturation using frequency-dependent rock physics models 83rd annual SEG meeting Expanded Abstracts, 3057-3061.

Xu, D., Wang, Y-H, Gan, Q. & Tang, J., 2011. Frequency-dependent seismic reflection coefficient for discriminating gas reservoirs. Journal of Geophysics and Engineering, 8, 508-513.

Zhang, S., Yin, X-Y & Zhang, G-Z, 2011. Dispersion-dependent attribute and application in hydrocarbon detection. Journal of Geophysics and Engineering, 8, 498.

Appendix I

Schoenberg and Protazio (1992) gave an explicit solution to the plane-wave reflection and transmission problem in terms of sub-matrices of the coefficient matrix of the Zoeppritz equation. Based on Schoenberg and Protazio (1992), Chapman and Liu (2003) derived the reflectivity, which is incident angle and azimuthal dependent. When fixing a polar angle and an azimuthal angle , the direction of propagation of the plane wave is $\mathbf{n}$ = (sin cos , sin sin , cos). Assuming a homogeneous incident P-wave travelling in cos , the axis normal to the interface is taken to be the direction $\mathbf{n}$. The velocity field of the incident wave will then be of the form:

$$v = i_0 \mathbf{e_p} expiw(\mathbf{s} \cdot \mathbf{x} - t)$$

where $\mathbf{e_p}$ is polarization and i_0 is the amplitude. The slowness of this wave is calculated as the value of $\sqrt{\ldots / t}$ having the smallest real part for is an eigenvalue of the matrix $C_{ijkl} n_i n_k$ and is the density of the rock. We then have $\mathbf{s} = \mathbf{n}$. The polarization is given by the eigenvector corresponding to . We now calculate expressions for the transmitted and reflected waves. Snell's law states that the horizontal slownesses of all waves interacting at the interface are equal. Since we know s_1 and s_2, the condition:

$$|C_{ijkl} s_i s_k - {}_{jl}| = 0$$

In both the upper and lower media gives a bicubic equation on the vertical slownesses. Solving for the admissible values of s_3, the polarizations, $\mathbf{e}$, satisfy the equation:

$$(C_{ijkl} s_i s_k - {}_{jl}) e_l = 0$$

and are obtained through singular value decomposition.

The required continuity of displacement and traction of the calculated waves give the conditions on reflected and transmitted amplitudes. Schoenberg and Protazio(1992) arranged the interface conditions into a convenient matrix representation. Specifically, the 3×3 reflection matrix R, is given by:
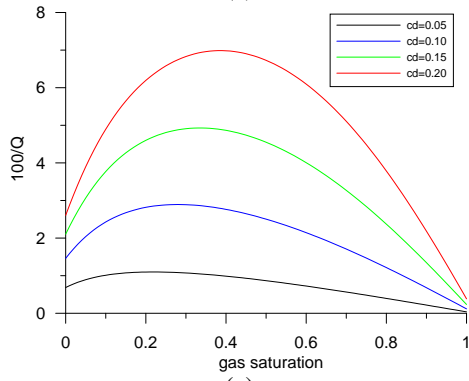
$$R = (X^{-1}X'-Y^{-1}Y')(X^{-1}X'+Y^{-1}Y')^{-1}$$

Where the matrices X, X', Y and Y' are as defined in Schoenberg and Protazio (1992), with the slownesses and polarizations taken from the above calculation. The PP reflection coefficient corresponding to the angles (,) is given by R_{11}.
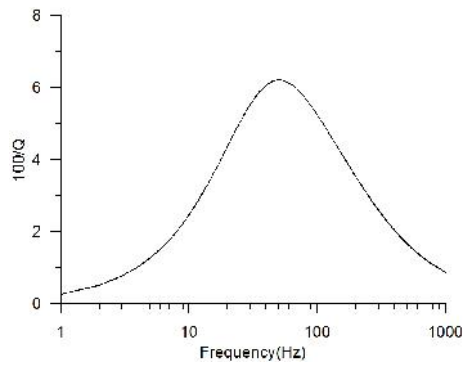
(a)
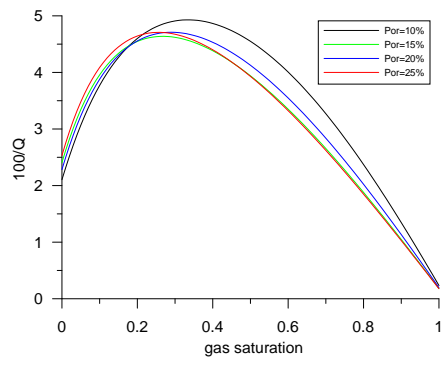
(b)

(c)

Figure 1 P-wave attenuation (100/Q) varying with (a) frequency; (b)gas saturation; (c)crack densities, predicted by the theory of Chapman et al. (2002). A crack density of 0.15 and porosity of 10% are given in (a). A crack density of 0.15 is given in (b). A porosity of 10% is given in (c). The values of attenuation peak at low gas saturation (about 20%) and go down to minimum values at full gas saturation. Attenuation also depends on crack density, which can be used for calibrating theoretical reflectivity to real data.
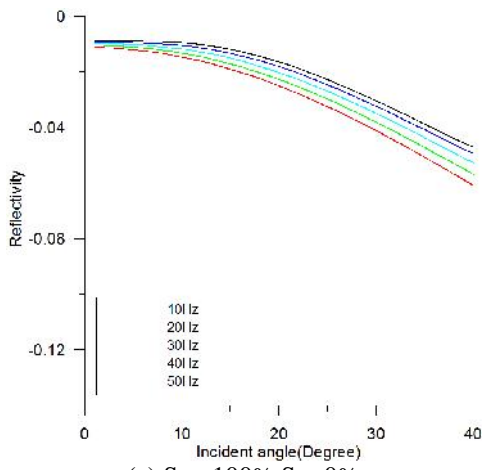
(a) Sw=100%,Sg=0%
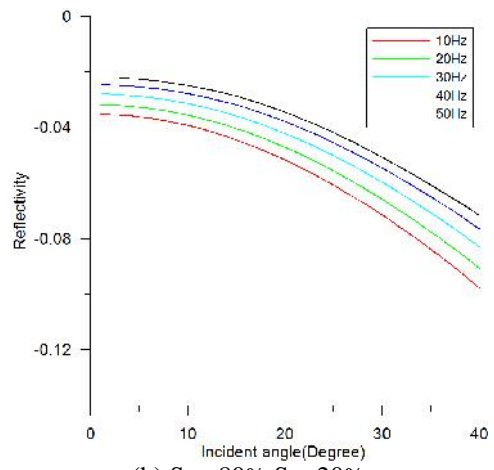
(b) Sw=80%,Sg=20%
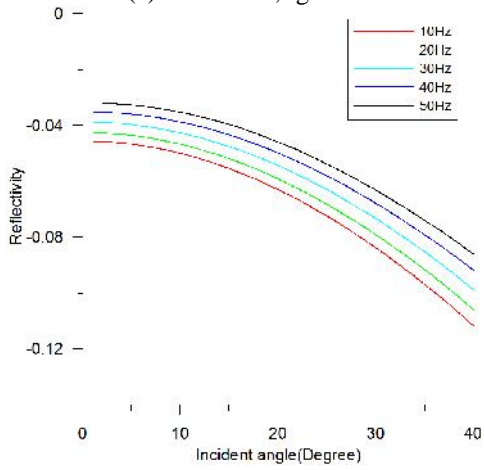
(c) Sw=60%,Sg=40%
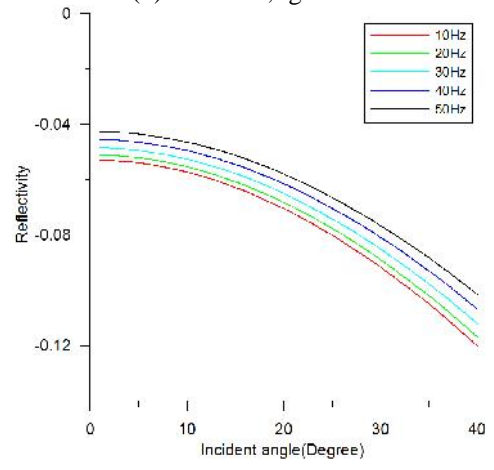
(d) Sw=40%,Sg=60%
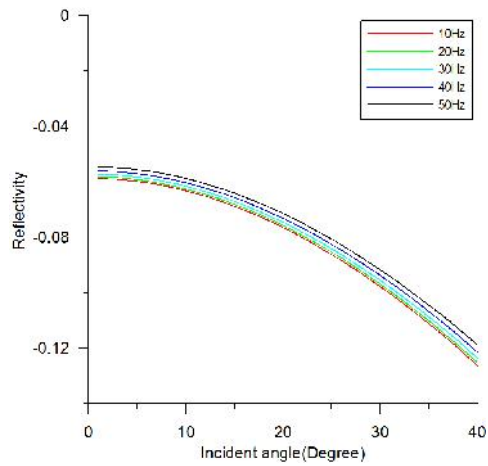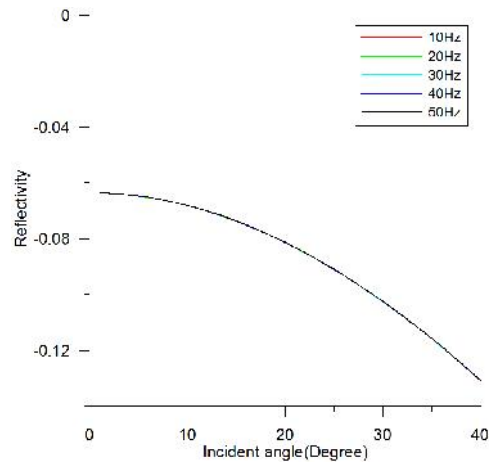
(e) Sw=20%,Sg=80%   (f) Sw=0%,Sg=100%

Figure 2. P-wave reflection coefficients as a function of incident angle for a series of frequencies when varying water saturation from 100% to 0%. The porosity is 10%. The maximum frequency-dependence of reflectivity occurs when gas saturation is 40%. High frequency-dependence of reflectivity is predicted for full water saturation while nearly frequency-independence for full gas saturation.
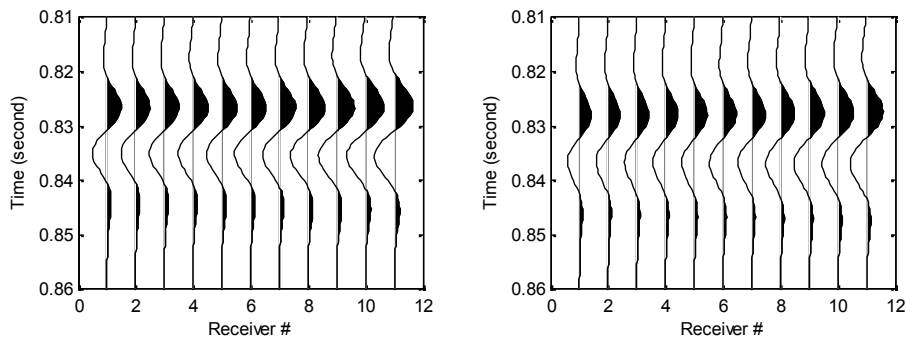

Figure 3 Synthetic reflection gathers at the interface for the two-layer model, with elastic layer (Left) and dispersive layer (Right) as the lower layer. Amplitudes exhibit Class III AVO feature for the two gathers. However, amplitudes for the dispersive model have decreased due to frequency-dependence of elastic impedance.
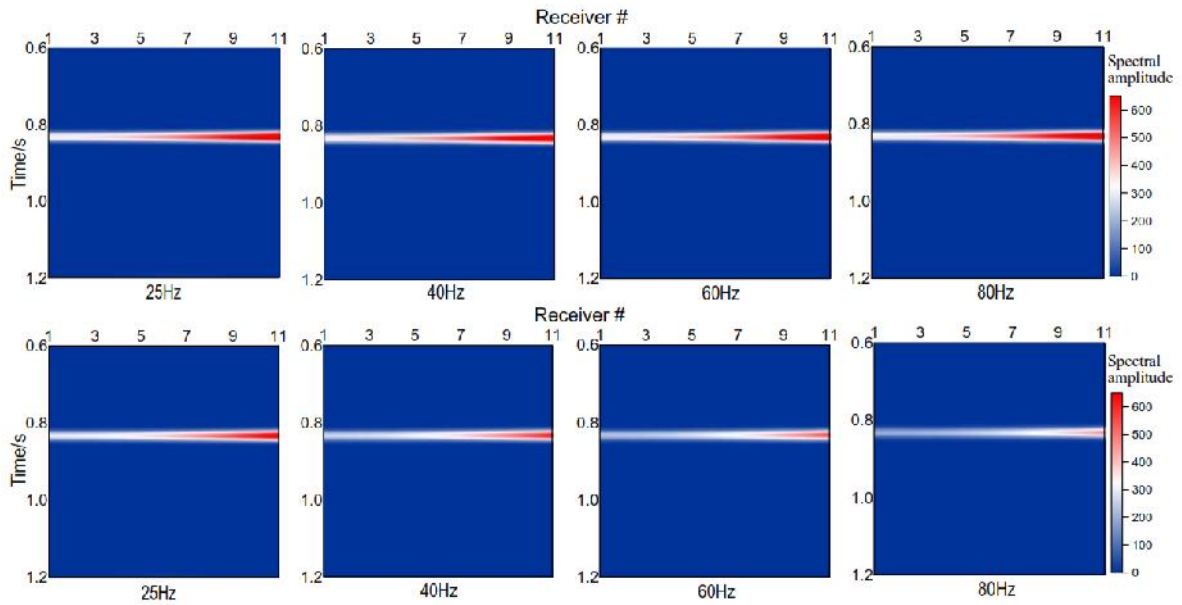
Figure 4 Isofrequency sections of (upper) the elastic gather and (lower) dispersive gather at 25Hz, 40Hz, 60Hz and 80Hz. Spectral balance based on the input wavelet has been carried out with 40Hz as reference frequency. For the elastic case, reflection energy conserved at different frequency. For the dispersive case, reflection energy decreases with increase of frequency.
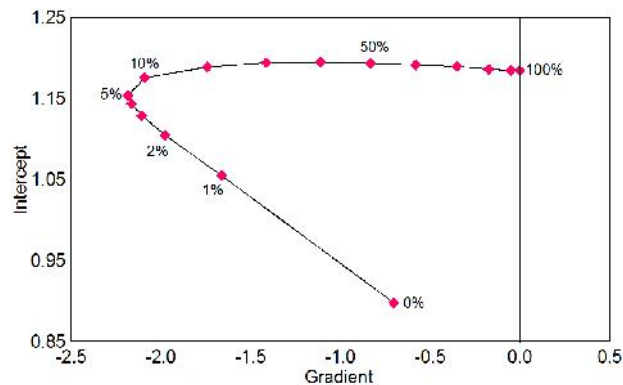

Figure 5: Crossplot of "low-frequency-reflectivity" (Intercept) versus "frequency-dependence of reflectivity" (Gradient). Values labelled near the pink squares refer to gas saturation. Large intercept and frequency-dependence occur around 5% gas saturation. Full water saturation has low intercept. Full gas saturation has nearly no frequency-dependence of reflectivity.
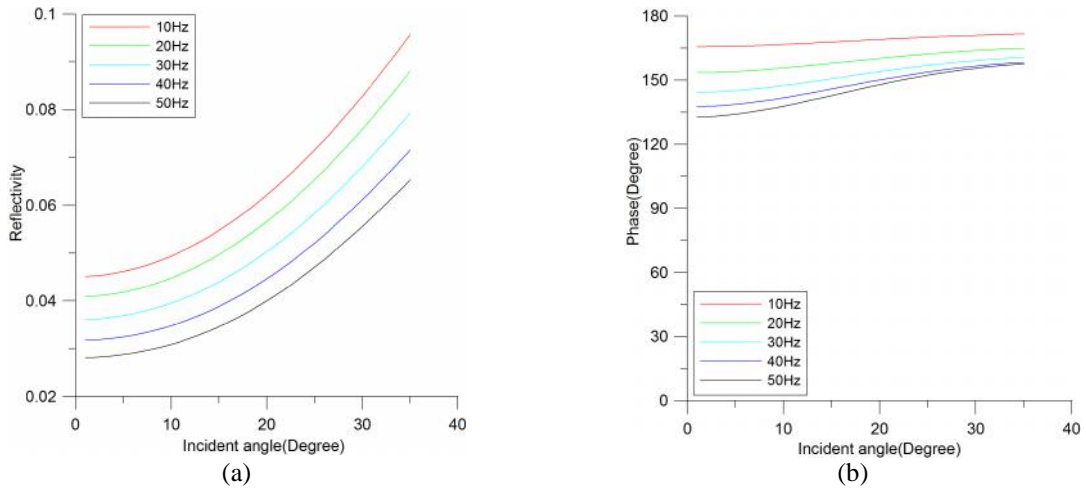
(a)   (b)

Figure 6. Frequency-dependent reflectivity (a) and phase (b) at the interface of the two-layer model, using Chapman et al.(2002) theory. The reflectivity does not contain phase information. The high-to-low interface gives rise to Class III AVO with phase around 180 degree.
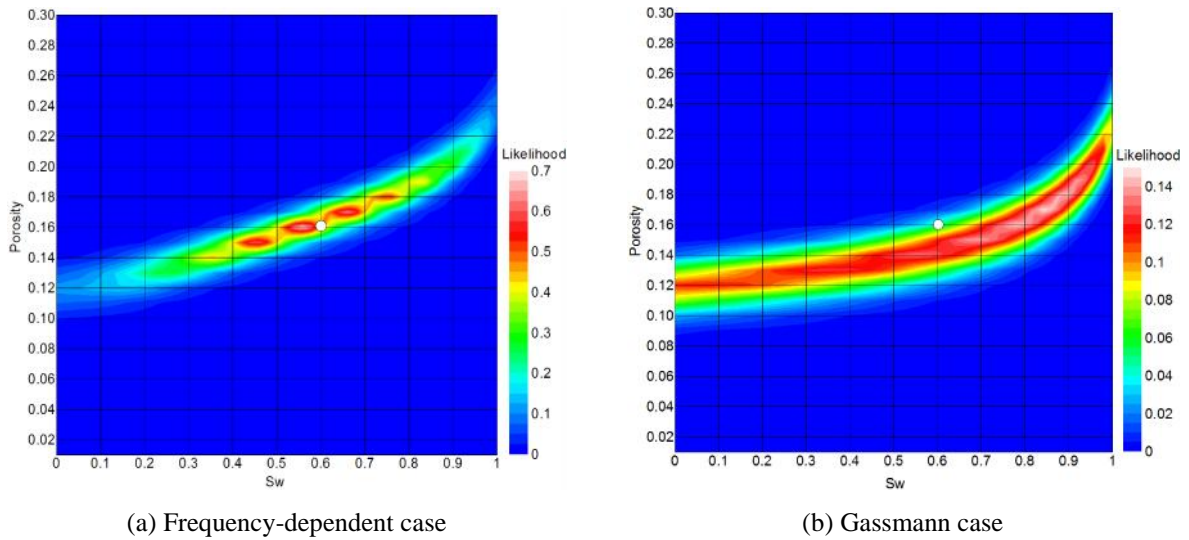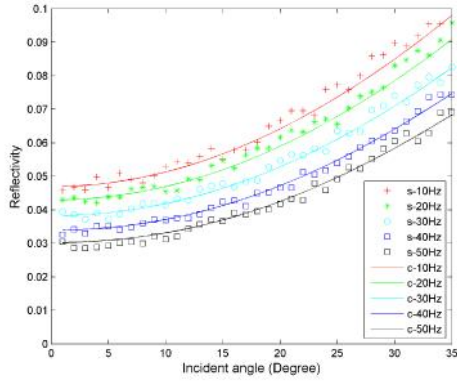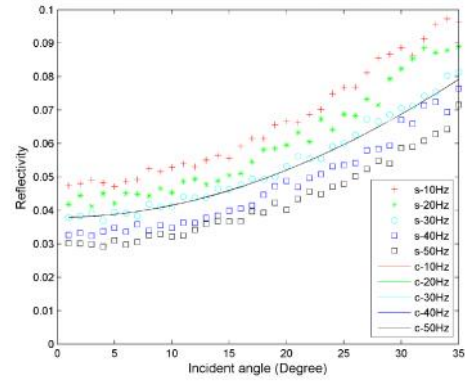

(a) Frequency-dependent case   (b) Gassmann case

Figure 7. Likelihood functions transformed from misfits between the theoretical reflectivity and the "observing data" using an exponential relation. Red and white colours represent highly likelihood of the porosity and water saturation to the true value. The true value of porosity (16%) and water saturation (60%) is labelled with white circle.

(a) Frequency-dependent case   (b) Gassmann case

Figure 8. The fitting results for the maximum likelihood of porosity and water saturation. For frequency-dependent case (a), $=16\%$, $S_w =55\%$ and for Gassmann case (b), $=17\%$, $S_w =85\%$. Symbols represent the "observing data", curves represent the modeling reflectivity.
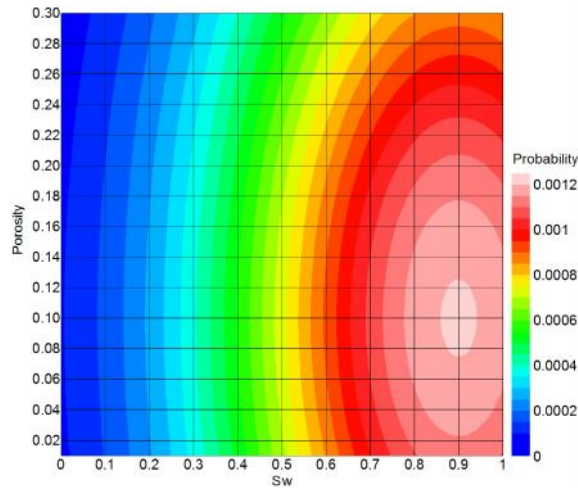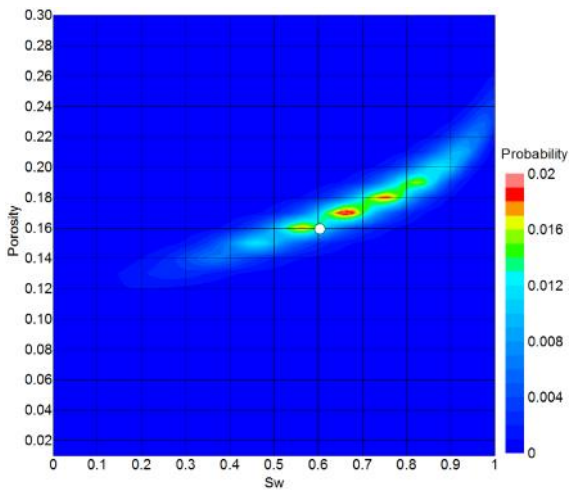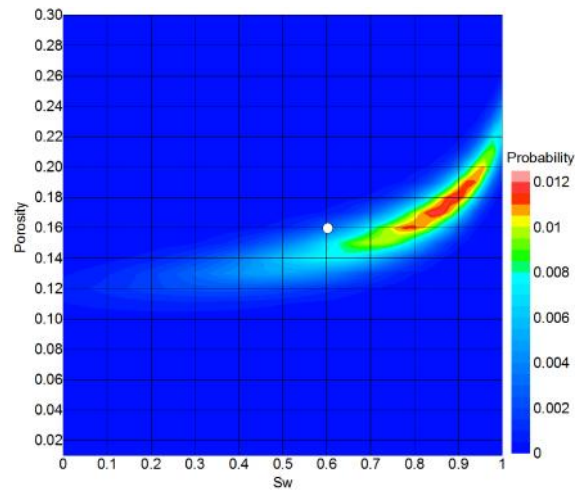

Figure 9. The prior information for porosity and water saturation. Both of the porosity and water saturation are assumed to be normally distributed, with mean value $\mu = 10\%$ and variance $^2 = 0.25$ for porosity, and $\mu = 90\%$ and $^2 = 0.25$ for water saturation.

(a) Frequency-dependent case   (b) Gassmann case

Figure 10 The posterior probability of porosity and water saturation for frequency-dependent case (a) and

Gassmann case (b). The true value of porosity (16%) and water saturation (60%) is labelled with white circle. The frequency-dependent case (a) provides more accurate estimation of porosity and water saturation.

Table 1 *The material parameters for the two-layer model with shales overlying sandstone reservoir.*

Layers	Vp(km/s)	Vs(km/s)	Vp/Vs	Den(g/cm^3)	Porosity	Crack density	Water saturation
Upper	3.200	1.600	2.0	2.50			
Lower	3.100	1.865	1.66	2.35	0.16	0.15	0.60

Table 2 *The material parameters for the two-layer model by Rutherford and Williams (1989)with shales overlying sandstone reservoir.*

Layers	Vp(m/s)	Vs(km/s)	Poisson ratio	Den(g/cm^3)	Porosity
Upper	4000	1760	0.15	2.4	
Lower	3800	2438	0.38	2.0	0.12